

Quantum Technology in Space

Robert Malaney

School of Electrical Engineering and Telecommunication
The University of New South Wales, Sydney, Australia

Presented at NASA HQ July 2025

Quantum Communications in Space

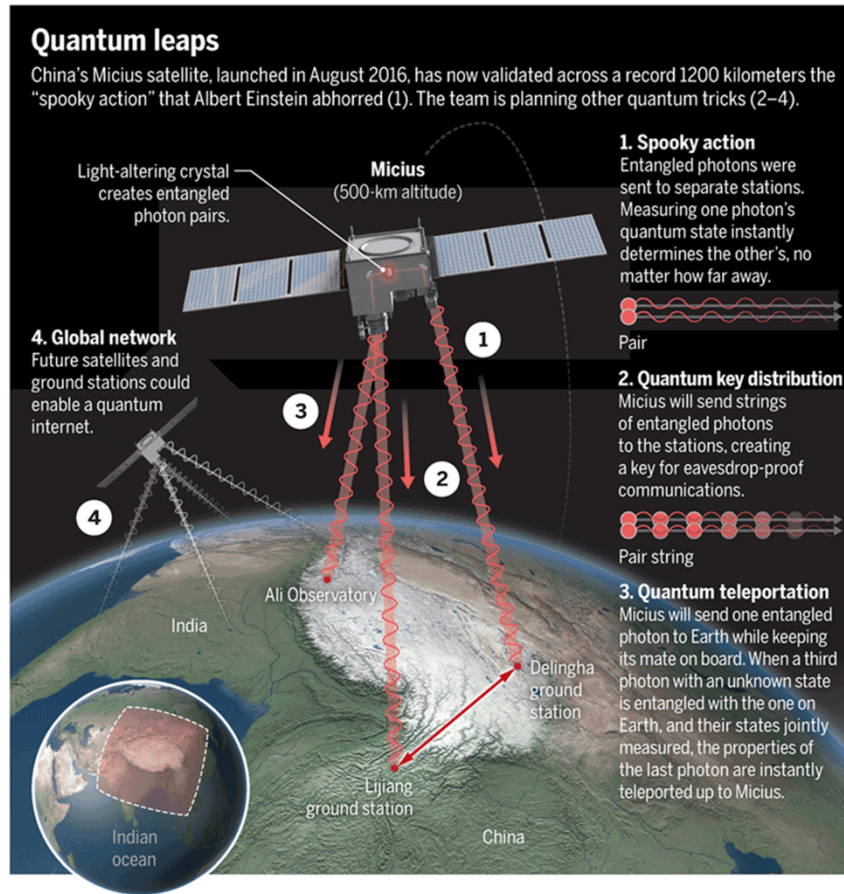
UNSW – Northrop Grumman 2018-2025

- **7 PhD Students, Two Postdocs**
- **30+ Published Papers (2 IEEE Best Paper awards)**
- **2 Patents**
- **1 Australian Research Council Linkage Grant - \$1m**
- **Collaboration with NASA Goddard (Mark Clampin, Peter Brereton, Holly Leopardi)**
- **New Quantum Satellite Prototype - \$2m**
(Northrop Grumman Australia – UNSW – Australian Government, Department of Defence)

The Quantum Internet

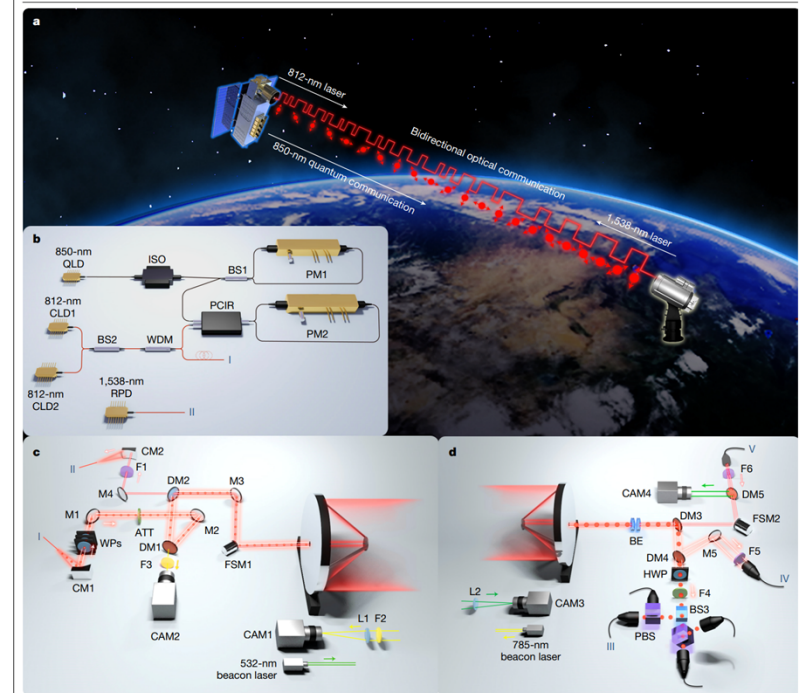
1. Why a Quantum Internet? Where are we at?
 2. Technical background for quantum information
 3. Why is quantum communication Earth to space hard?
 4. Some new ideas that may help
 5. Securing quantum information (including sensing data)
 6. Quantum Internet- what is next ?
-
7. Sensing with the Quantum Internet.....
.....Beating the standard quantum limit (SQL->HL)

Quantum Internet- Where are We?



Where are we?

- One large (**500kg**) deployed system (2017)
–one **23kg** satellite (2025)
- Many others planned (e.g. Eagle-1))



Article

Microsatellite-based real-time quantum key distribution

<https://doi.org/10.1038/s41586-025-08739-z>

Received: 29 July 2024

Accepted: 4 February 2025

Published online: 19 March 2025

Check for updates

Yang Li^{1,2,3,4}, Wen-Qi Cai^{1,2,3,4}, Ji-Gang Ren^{1,2,3,4}, Chao-Ze Wang^{1,2,3}, Meng Yang^{1,2,3}, Liang Zhang^{3,4}, Hui-Ying Wu³, Liang Chang⁵, Jin-Cai Wu^{1,4}, Bao Jin⁶, Hua-Jian Xue^{1,2,3}, Xue-Jiao Li^{1,2,3}, Hui Liu⁶, Guang-Wen Yu^{1,2,3}, Xue-Ying Tao^{1,2,3}, Ting Chen⁶, Chong-Fei Liu^{3,4}, Wen-Bin Luo^{1,2,3}, Jie Zhou⁶, Hai-Lin Yong⁶, Yu-Huai Li^{1,2,3}, Feng-Zhi Li^{1,2,3}, Cong Jiang⁷, Hao-Ze Chen⁸, Chao Wu⁹, Xin-Hai Tong⁹, Si-Jiang Xie⁹, Fei Zhou⁹, Wei-Yue Liu^{1,2,3}, Yaseera Ismail^{10,11}, Francesco Petruccione^{10,11,12}, Nai-Le Liu^{1,2,3}, Li Li^{1,2,3}, Feihu Xu^{1,2,3}, Yuan Cao^{1,2,3}, Juan Yin^{1,2,3}, Rong Shu^{1,4}, Xiang-Bin Wang⁷, Qiang Zhang^{1,2,3,7}, Jian-Yu Wang^{1,4}, Sheng-Kai Liao^{1,2,3,10}, Cheng-Zhi Peng^{1,2,3,10} & Jian-Wei Pan^{1,2,3,10}

What is to be done?

- Rates, DI-QKD, Networking, CV
- **Synchronisation (& secured), and**
- **QKD's BIG problem**

Quantum Communications

Quantized Electromagnetic Field

(This is all you ever need to knowto 99% level)

Quantwiki.org



Source free

$$\nabla \times \mathbf{E} + \frac{\partial \mathbf{B}}{\partial t} = 0$$

$$\nabla \cdot \mathbf{E} = 0$$

$$\nabla \cdot \mathbf{B} = 0$$

$$\nabla \times \mathbf{B} - \epsilon \mu \frac{\partial \mathbf{E}}{\partial t} = 0$$

$$\mathbf{E}(r, t) = \sum_{k,s} E_k \mathbf{e}_k^{(s)} \left[\alpha_{k,s} e^{i(kr - \omega_k t)} + \alpha_{k,s}^* e^{-i(kr - \omega_k t)} \right]$$

$$E_k = \left(\frac{\hbar \omega_k}{4\pi \epsilon_0} \right)^{1/2}$$

Promote Fourier components $\alpha_{k,s}$ to operators $\hat{a}_{k,s}$

The classical \mathbf{E} field is the expectation value of the quantum operator $\hat{\mathbf{E}}$



wattsupwiththat.com

$$\begin{aligned} [\hat{a}_{k,s}, \hat{a}_{k',s'}^\dagger] &= \delta_{kk'} \delta_{ss'}, \\ [\hat{a}_{k,s}, \hat{a}_{k',s'}] &= 0 \\ [\hat{a}_{k,s}^\dagger, \hat{a}_{k',s'}^\dagger] &= 0 \end{aligned}$$

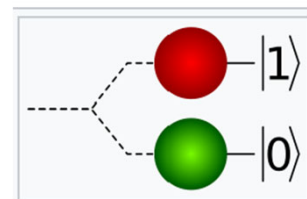
$$\hat{\mathbf{E}}(r, t) = E_0 \mathbf{e} \left[\hat{X} \cos(kr - \omega t) + \hat{P} \sin(kr - \omega t) \right]$$

$$\hat{X} = \frac{1}{\sqrt{2}} (\hat{a} + \hat{a}^\dagger)$$

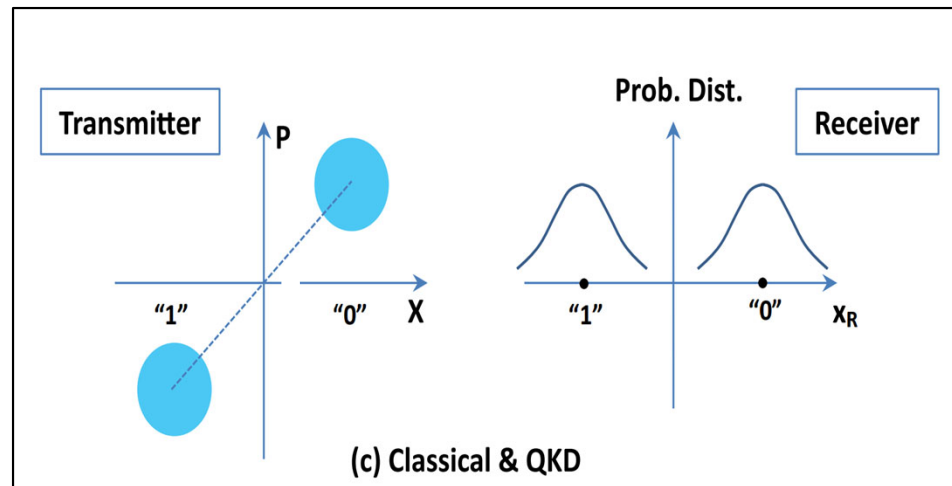
$$\hat{P} = \frac{1}{\sqrt{2}} (\hat{a} - \hat{a}^\dagger)$$

$$|\psi\rangle = \alpha|0\rangle + \beta|1\rangle$$

$$|\alpha|^2 + |\beta|^2 = 1$$

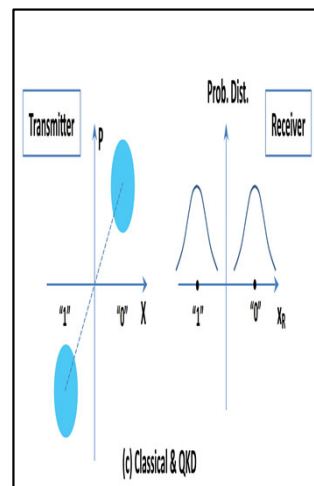


Classical and Quantum Comms with Lasers



$$[\hat{X}, \hat{Y}] = 2i.$$

$$\langle \Delta^2 \hat{X} \rangle \langle \Delta^2 \hat{Y} \rangle \geq \frac{1}{4} |[\hat{X}, \hat{Y}]|^2 = 1.$$



Quantum Sensing:

Definition of a mode from Maxwell's equations

A **mode** is a normalized solution of the following equations:

Maxwell's equations in volume V

$$\left(\nabla^2 - \frac{1}{c^2} \frac{\partial^2}{\partial t^2} \right) f(\vec{r}, t)$$

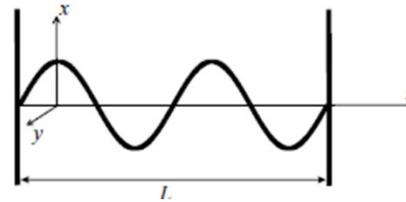
$$= 0$$

$$\nabla \cdot f(\vec{r}, t) = 0$$

Examples of modes: polarization, frequency, spatial and temporal.

$$\frac{1}{V} \int_V |f(\vec{r}, t)|^2 d^3\vec{r} = 0$$

E field in cavity with conducting walls



E field decomposed into modes, f_m

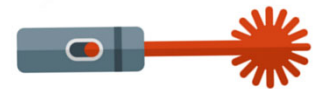
$$E^{(+)}(\vec{r}, t) = \sum_m \epsilon_m f_m(\vec{r}, t)$$

$$E(\vec{r}, t) = E^{(+)}(\vec{r}, t) + E^{(-)}(\vec{r}, t)$$

$$E^{(-)}(\vec{r}, t) \equiv \left(E^{(+)}(\vec{r}, t) \right)^*$$

$$\epsilon_m = \sqrt{\frac{\hbar \omega_m}{2 \epsilon_0 V}}$$

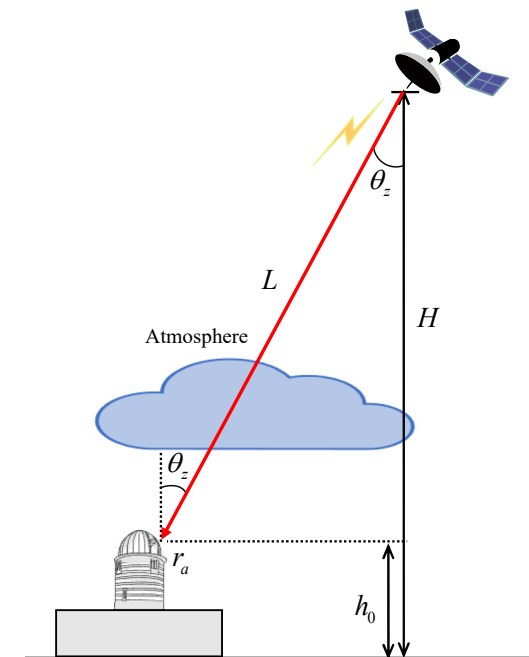
$$\vec{r} = (x, y, z)$$



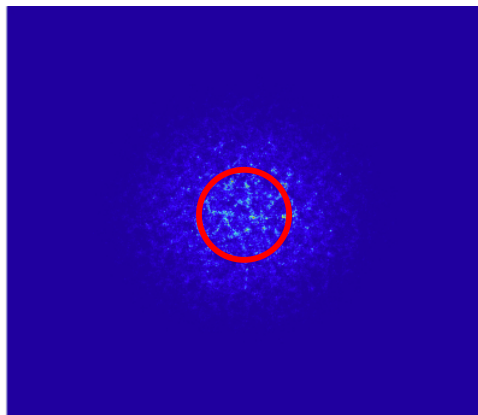
Building the Quantum Internet is Hard!

Global quantum Internet needs both downlink (Earth-to-satellite) and uplink (i.e., Earth-to-satellite) channels.

- Downlink channels are predominately used: dominated by
- diffraction loss (pseudo-fixed).
 - just increase receiver aperture size...
- **Uplink channels are sometimes preferred** to downlink
- channels when considering
 - 1) limitation of resources (e.g., entanglement) at satellite and
 - 2) flexibility of ground-station systems.

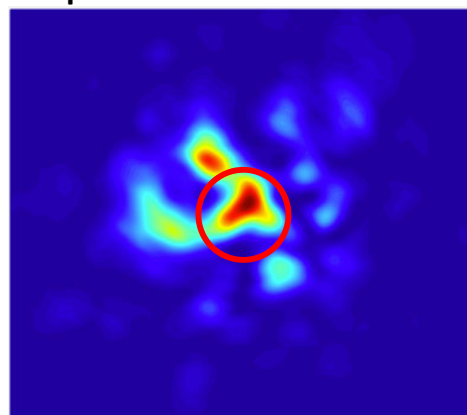


Downlink Beam

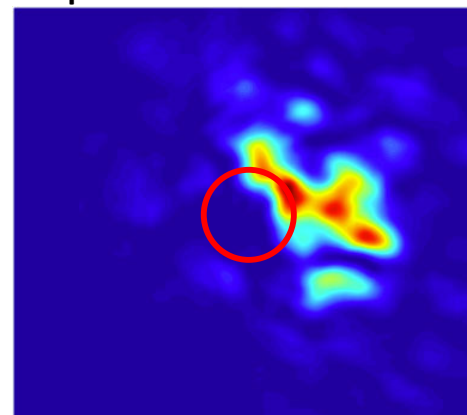


diffraction-loss dominated (wang et al)

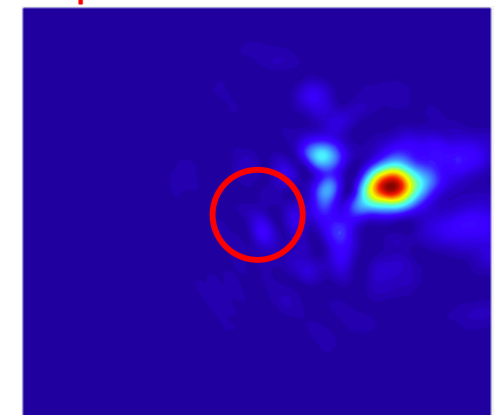
Uplink Beam: Realization 1



Uplink Beam: Realization 2



Uplink Beam: Realization 3

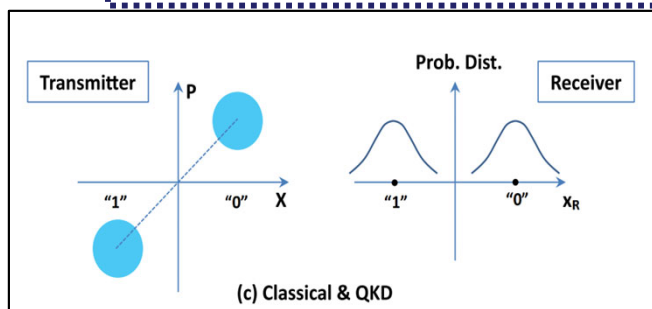
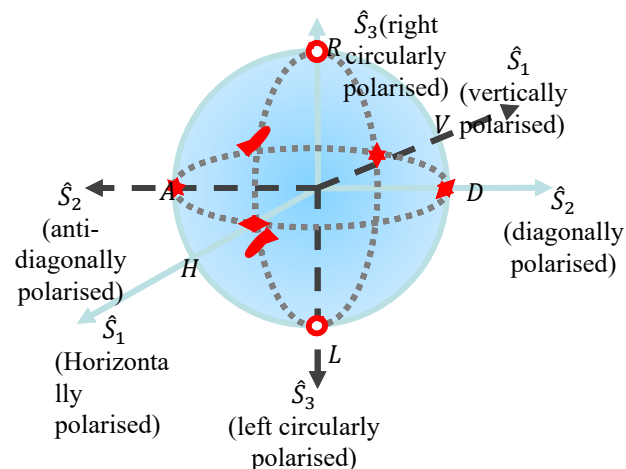
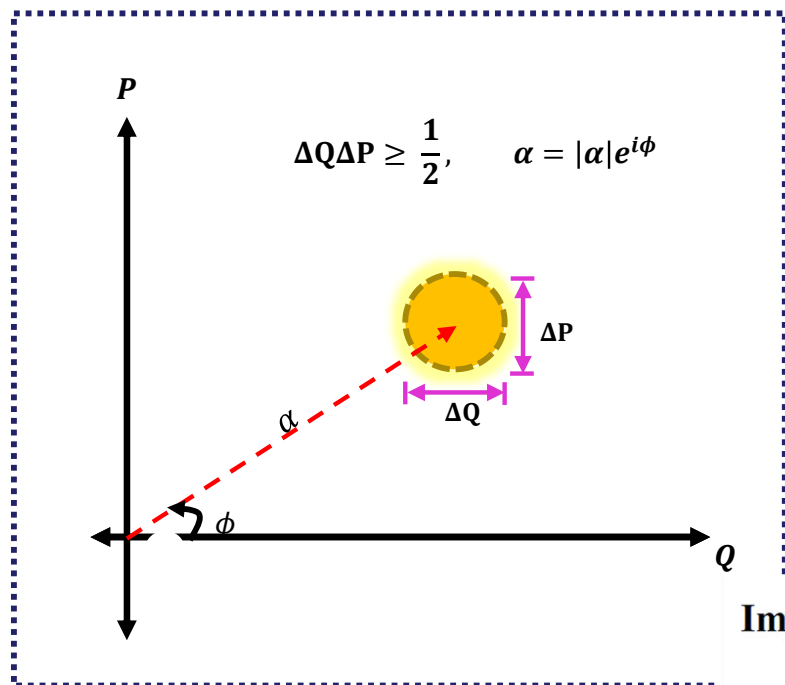


Rx aperture gets almost nothing!

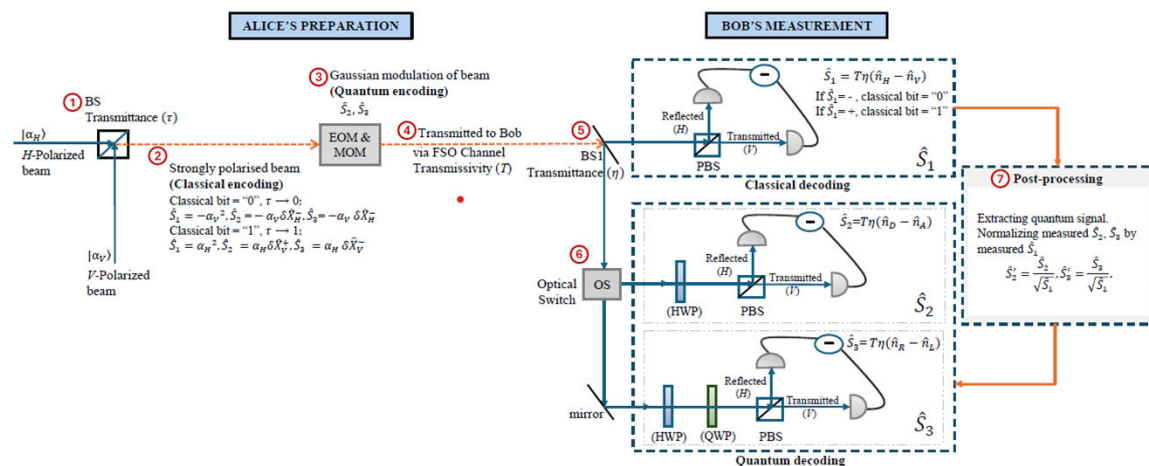
Classical-Quantum Signalling via Stokes Parameters

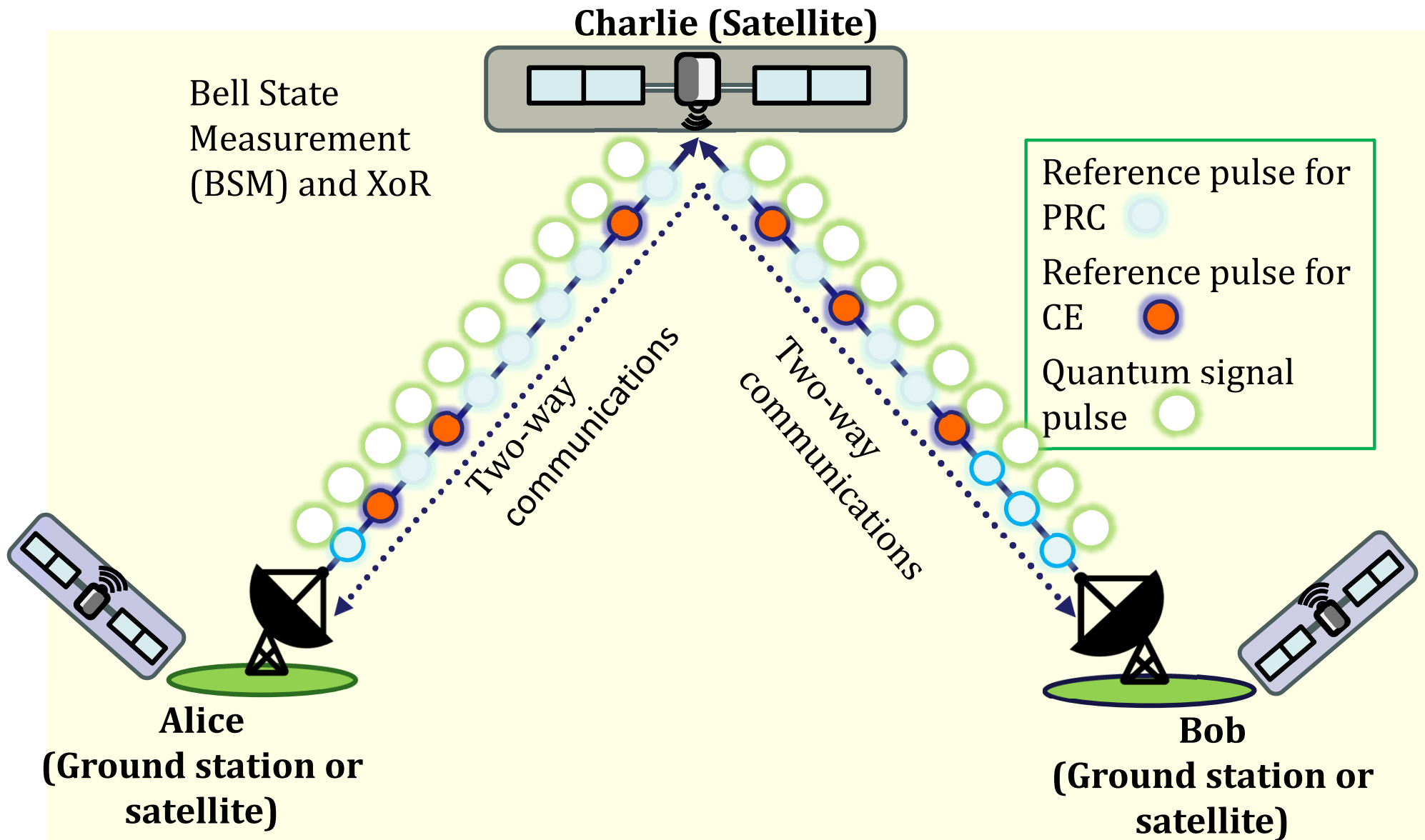
Best Paper Award, IEEE Globecom 2024, Cape Town, S. Africa.

Anjali Dhiman, et al (ARC Linkage)



Implementation of Stokes-based SQCC protocol





Spatial Diversity in the Uplink

Wang et al (2025) DOI 10.1109/TCOMM.2025.3573448

Diversity: send and/or receive same symbols over separate (physically or virtually) subchannels.

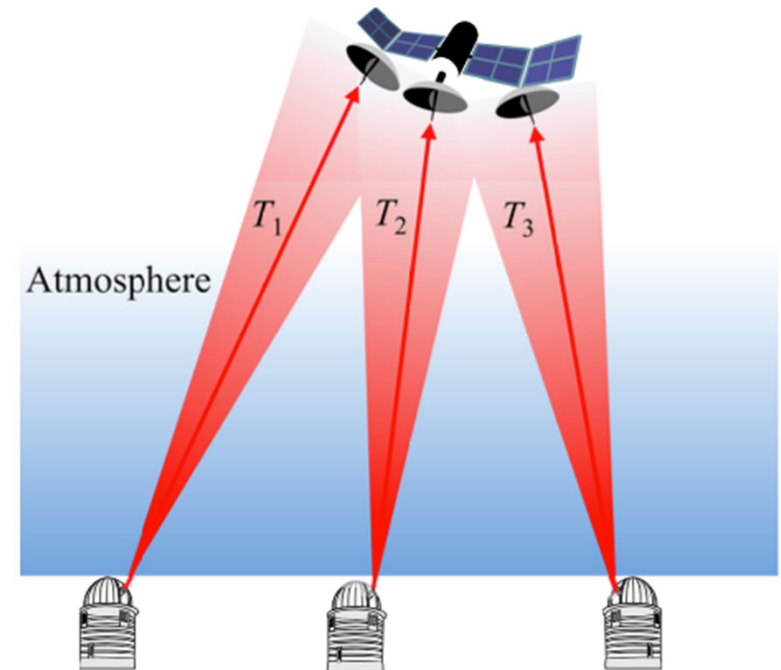
- Requirement: subchannels are (at least partially) independent.
- Effect: probability of deep fades reduced (by properly combining subchannel signals).

Spatial diversity: employing multiple transmitters and/or receivers.

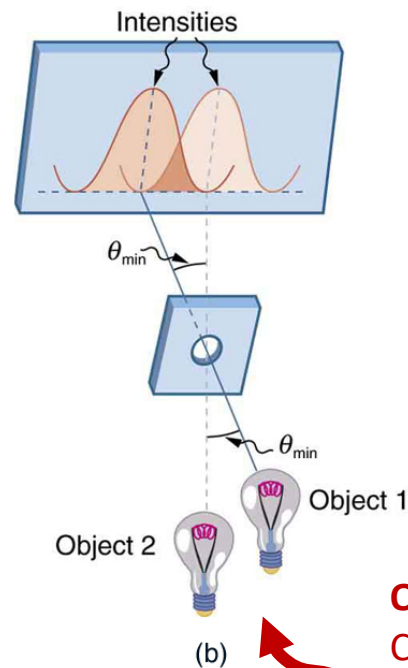
- Wireless Communications: exploits *multipath propagation*.
- Optical Communications: creates *channel independence* via **physical separation of subchannels**.
 - Readily achieved by **separating transmitting telescopes** by a reasonable distance.
 - Atmospheric *coherence length* of near-ground local atmosphere (i.e., several kilometers up into an uplink channel) is on the order of centimeters!

Practical setting to introduce diversity

- M transmitting ground stations
- Single receiving satellite with M receiving apertures
- One ground station tracks one receiving aperture
 - $\rightarrow M$ independent random subchannels
- No channel information @ Tx
 - \rightarrow all ground stations send the same quantum state
- Channel loss information @ Rx
 - \rightarrow optimal combining @ satellite

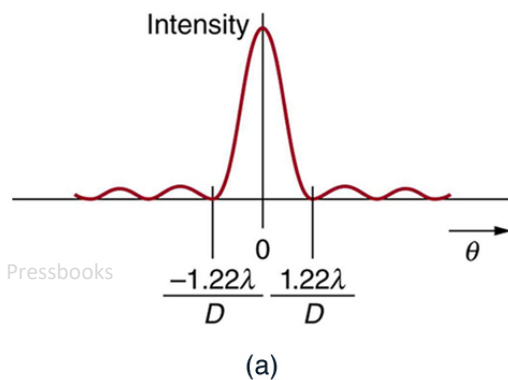


Defeating Rayleigh's Curse with Quantum Measurements

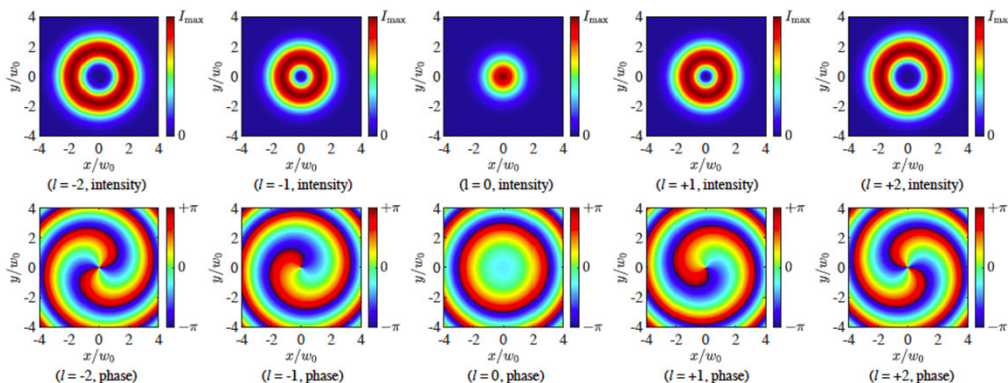


Aim:

Rayleigh curse defeated for
angle jitter less than
one part in a million



Quantum Measurement:
Count Number Photons in each
Hermite-Gaussian Modes (SPADE)



GOSALIA ET AL (NASA COLLABORATION)

Entanglement Based Quantum Key Distribution System

- **EPS Source (Satellite)** – Distribute entangled photons among two ground stations on earth.
- The photons travel through a **lossy** channel.
- **Alice** (Ground station) and **Bob** (Ground station) receive the photons and perform the measurements in different polarization basis and detect the photons using **single photon detectors**.

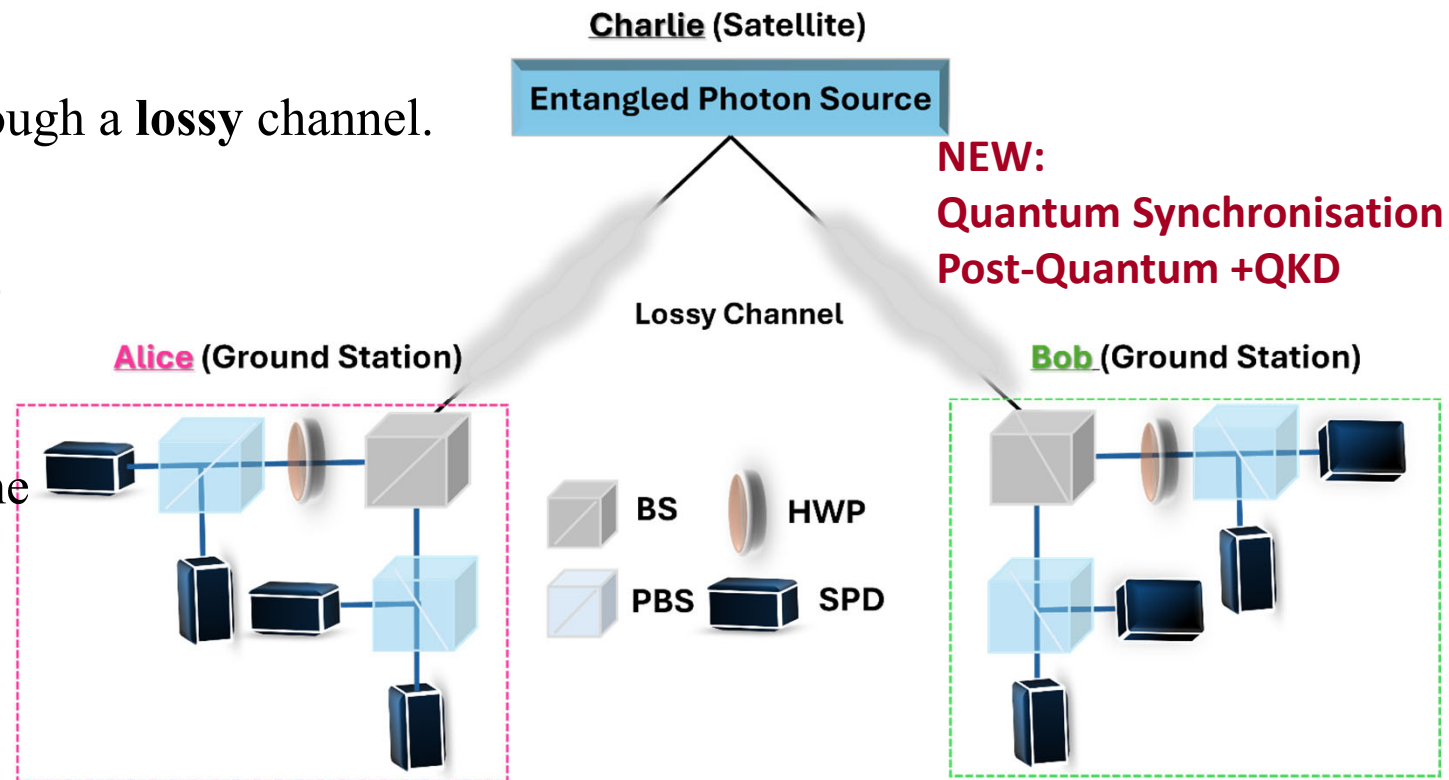
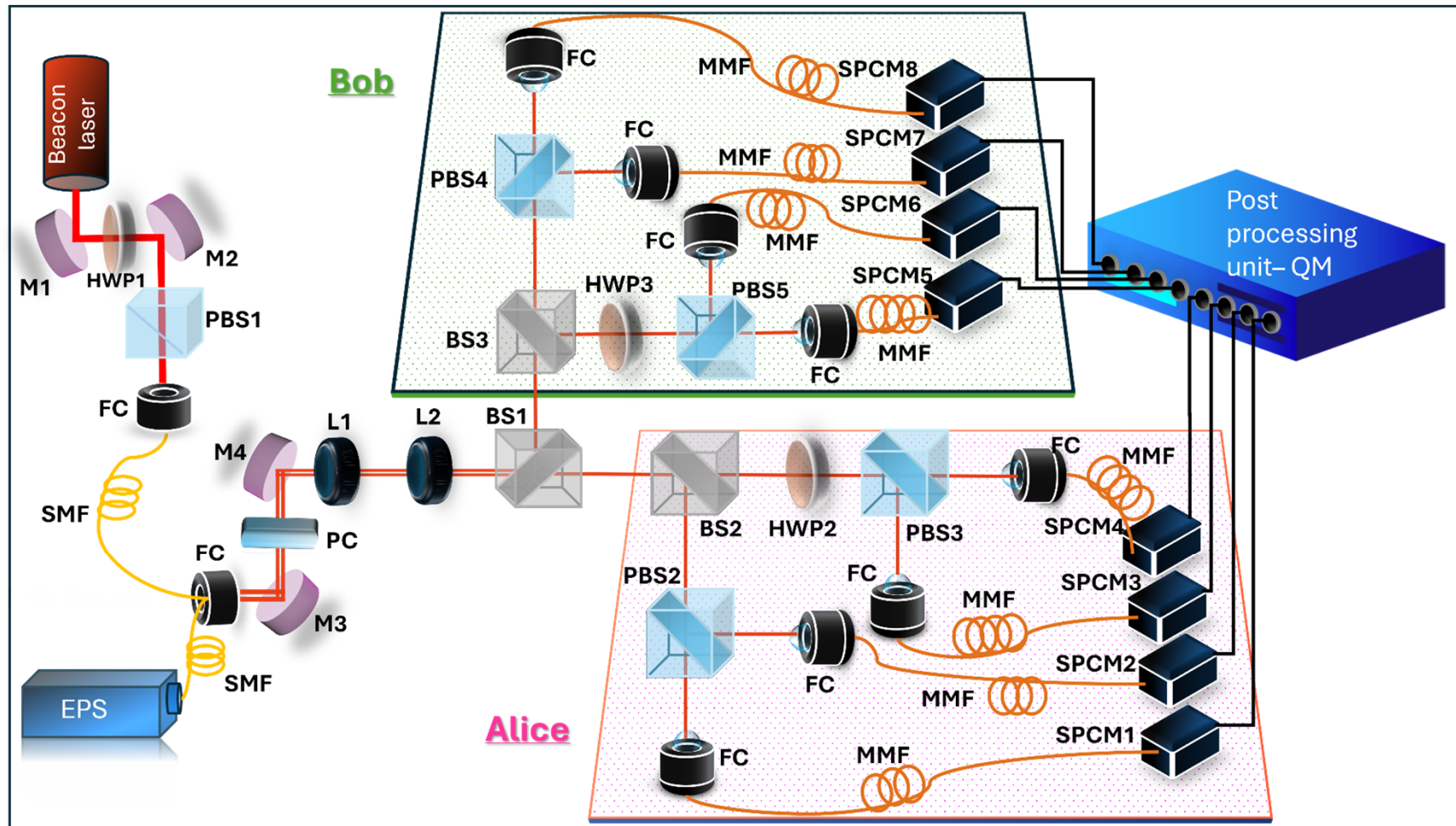


Figure. Entanglement-based satellite quantum communication system. HWP: Half-wave plate; PBS: Polarizing beam splitter; SPD: Single-photon detector; BS: Beam splitter.

Experimental Setup for BBM92 Protocol



EPS: Entangled photon source; M: Mirror; HWP: Half-wave plate; PBS: Polarizing beam splitter; FC: Fiber coupler; SMF: Single-mode fiber; PC: Polarization correction optics which is a combination of a quarter-wave plate - half-wave plate - quarter-wave plate; BS: Beam splitter; L: Lens; MMF: Multi-mode fiber; SPCM: Single-photon counting module; QM: Quantum machine (post-processing unit).

A Source for the Quantum Internet?

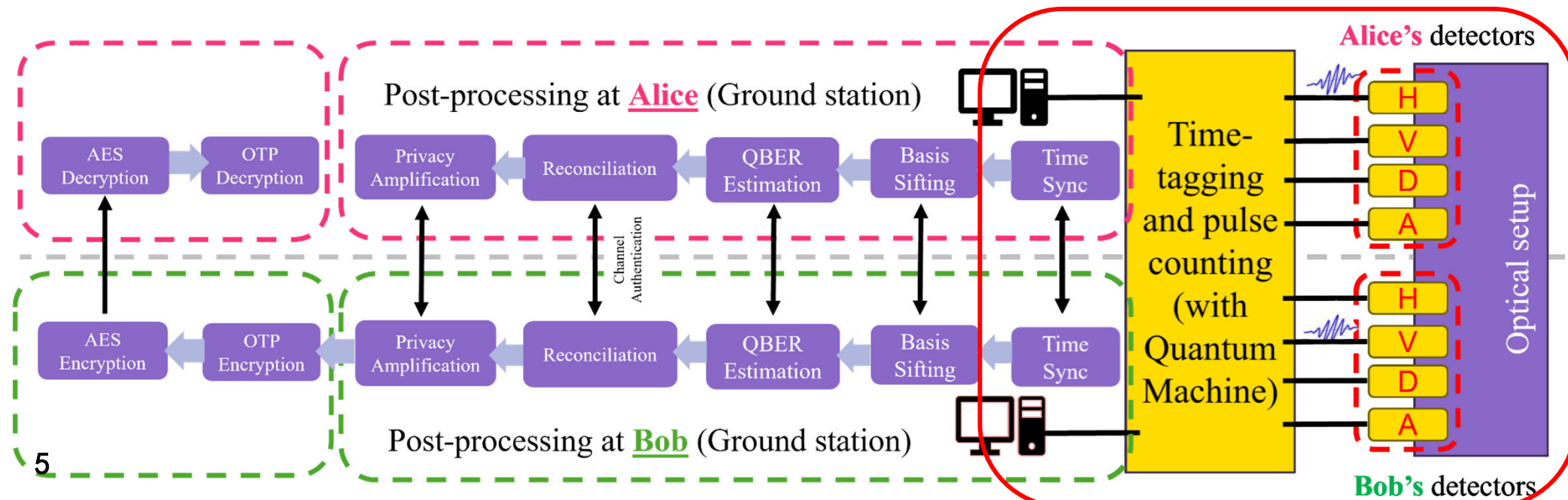
- A beacon laser is used for the coarse alignment for Alice and Bob's setup.
- The EPS source generates two entangled photons polarized in H and V. The entangled state is given by the expression,

$$|\psi\rangle = \frac{|H\rangle_s |V\rangle_i + |V\rangle_s |H\rangle_i}{\sqrt{2}}$$

- Alice and Bob perform the measurement in different polarization bases and detect the photons using single photon detectors at both ends.
- The photons are correlated in time, and only those photons will contribute to the key which are received at the same time towards both ends.
- Alice and Bob then filter the basis and perform the post-processing, which includes error estimation, reconciliation, and privacy amplification.

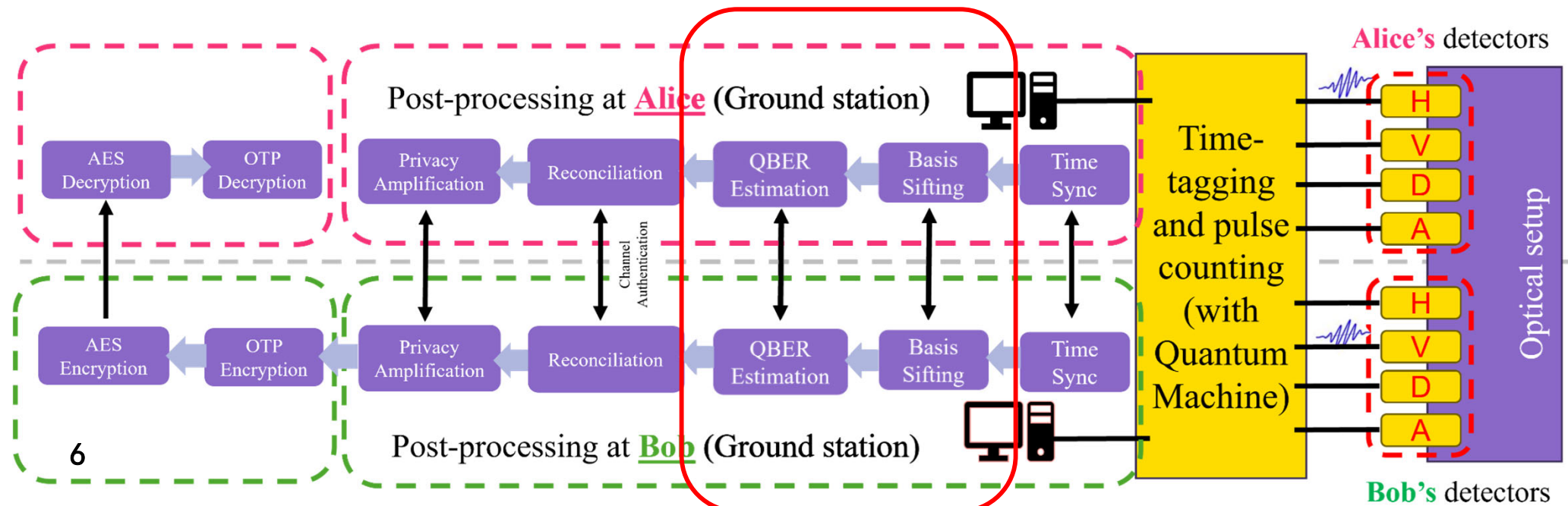
QKD Post-Processing

- Photon Time-tagging and filtering
 - A dedicated device monitoring all the 8 channels records the exact time (i.e. time tags) in ns when each detector sees a photon.
 - Keep the time tags only if the time difference between the Alice's and Bob's detections is less than 1 nanosecond.
 - This removes random noise from background light.



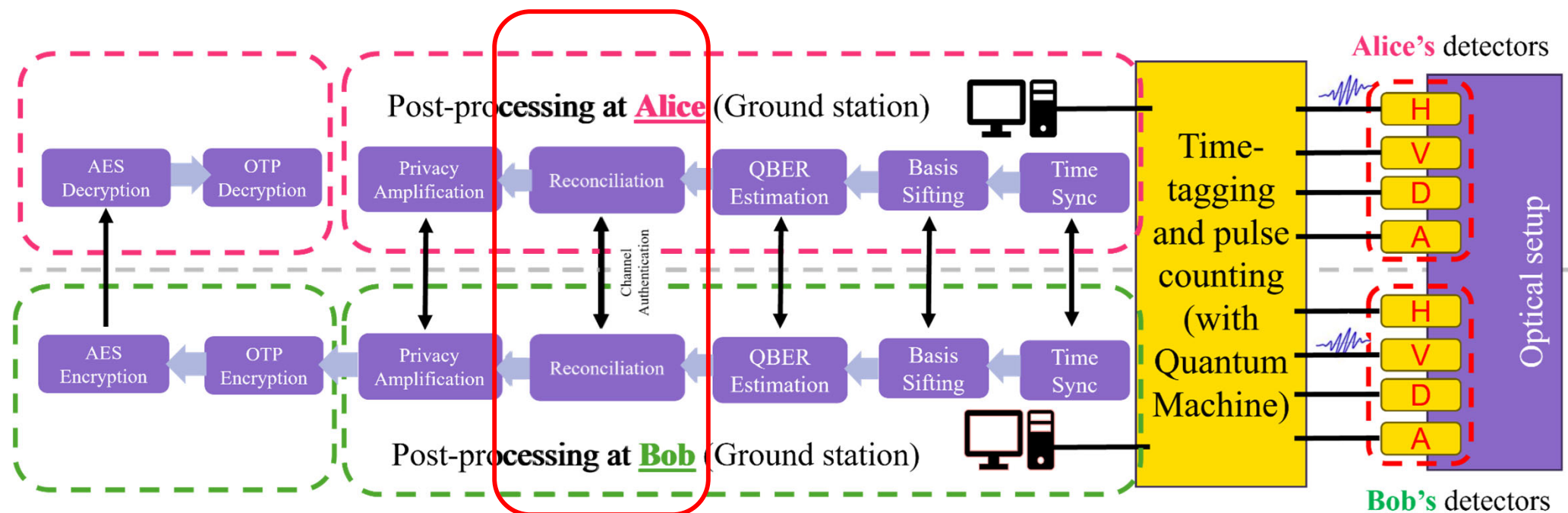
QKD Post-Processing

- Bit Mapping, Sifting and QBER Estimation
 - Generate raw key bits based on BB84 polarisation encoding
 - Raw key bits are kept only when Alice and Bob used the same measurement basis.
 - Alice shares some bits with Bob to estimate how many errors occurred in the transmission.



QKD Post-Processing

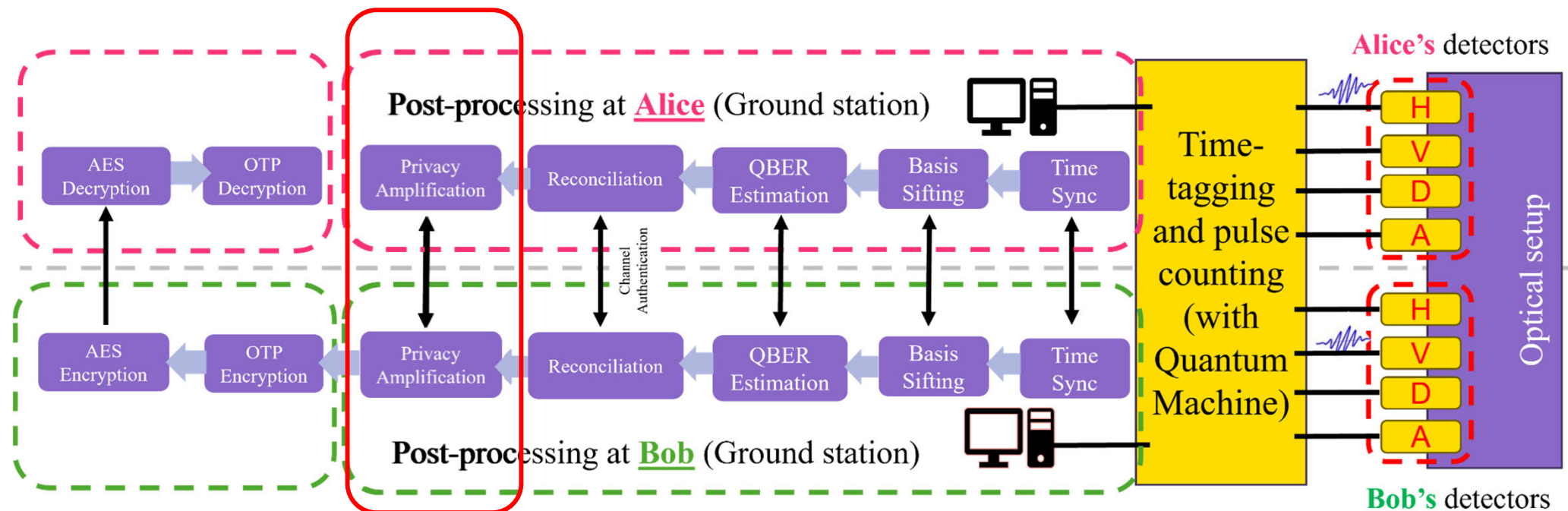
- Reconciliation on authenticated channels
 - Reconciliation based on special LDPC codes optimised for DV-QKD.
 - Authentication: Information theoretic Wegman Carter Message Authentication Codes with fixed pre-shared keys and logarithmic size QKD keys.



QKD Post-Processing

- Privacy Amplification

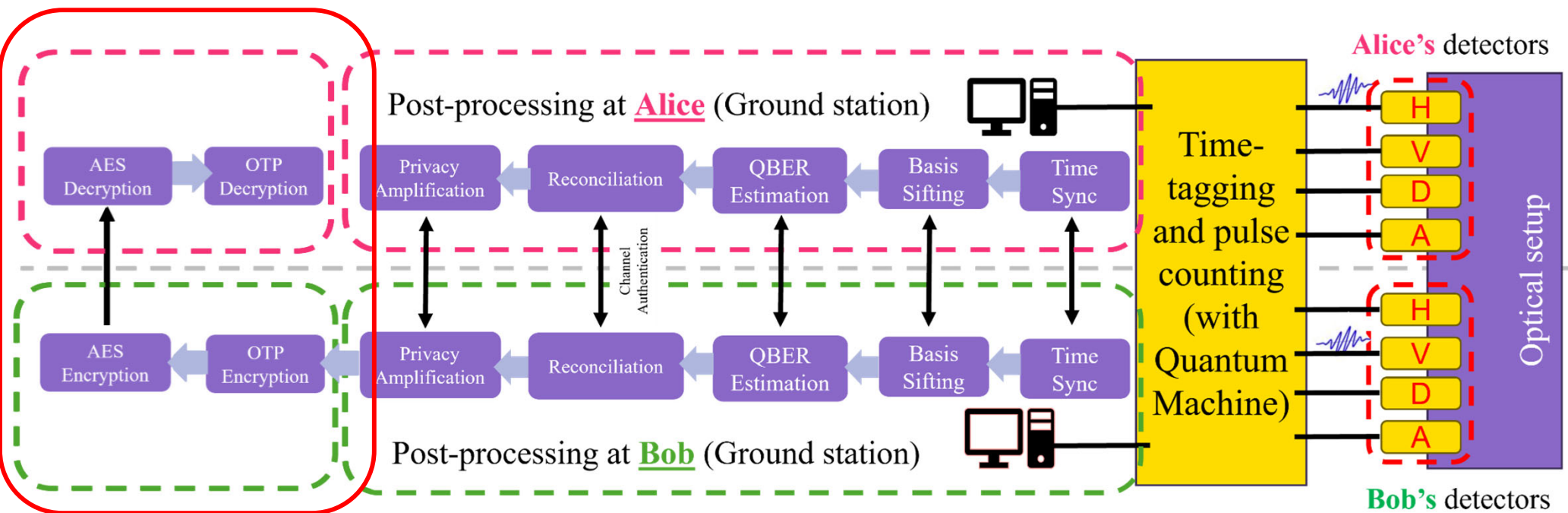
- Generate QKD secret keys based on asymptotic security analysis
- QKD keys are saved in a key pool for authentication and message encryption/decryption.



QKD+PQC Communications

- Hybrid Encryption-Decryption

- Double encryption and decryption of communication message performed in this architecture.
 - First, OTP encryption with QKD keys
 - The output is encrypted again with AES256, which is considered post-quantum secure.
- In case of running out of QKD keys, post-quantum security is ensured with AES.



QKD+PQC Architecture

- Hybrid Encryption-Decryption

Encryption Algorithm

```
if  $|K_q| \geq |M|$ :  
     $out \leftarrow K_q \oplus M$   
else:  
     $out \leftarrow M$   
 $out \leftarrow AES256\_Enc(K_a, out)$   
end
```

out

Decryption Algorithm

```
 $out \leftarrow AES256\_Dec(K_a, enc\_M)$   
if  $|K_q| \geq |M|$ :  
     $M \leftarrow K_q \oplus out$   
else:  
     $M \leftarrow out$   
end
```

- K_q is the shared QKD keys.
- K_a is pre-shared keys
- M is message and enc_M is encrypted message.
- $AES256_Enc$ is 256-bit AES encryption algorithm and $AES256_DEC$ is corresponding decryption algorithm.
- $|\cdot|$ represents the length of element `.`

- Information Theoretic security (post-quantum security) in worst case.
- Non-similar QKD and PQC keys are allowed.
- Compossible security analysis in not needed.

Emulating Earth-Satellite Channels

Key Equation:

The free-space channel loss, including beam diffraction, optical losses in the telescopes, and pointing loss, is given by:

$$A_{fs} = 10 \log_{10} \left(\frac{L^2 \lambda^2}{D_T^2 D_R^2 T_T T_R (1 - P_l)} \right)$$

Where:

- L = Link distance
- λ = Operating wavelength
- D_T, D_R = Transmitter and receiver telescope diameters
- T_T, T_R = Transmission efficiency of telescopes
- P_l = Pointing loss

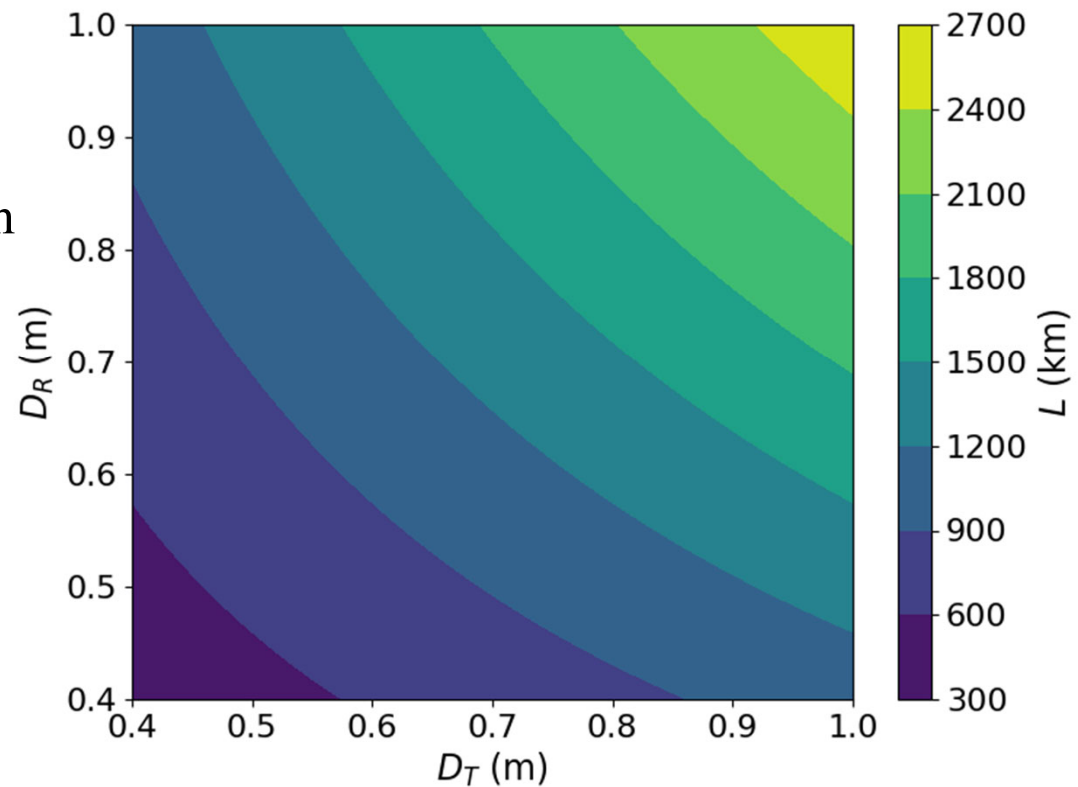


Fig. Plot of link distance L as a function of transmitter (D_T) and receiver (D_R) telescope diameters for fixed link loss of 10.3 dB, $\lambda = 800$ nm, $P_l = 0.2$, and $T_T = T_R = 0.8$.

Experimental Results

- Live **QBER (Q)** is plotted with time.
- QKD **key rate** in bits per pulse, **r** is calculated using eq.,

$$r = 1 - h(Q) - leak_{EC}$$

where,

$$h(x) = -(1-x)\log(1-x) - x\log(x)$$

$leak_{EC}$ - is the information leakage

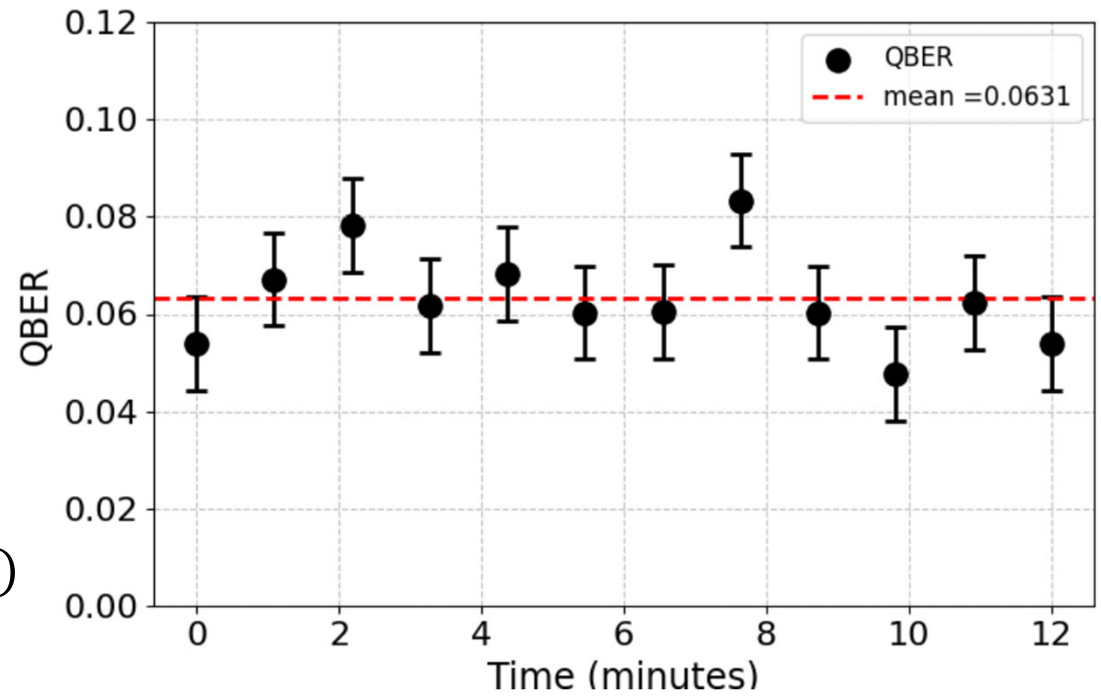
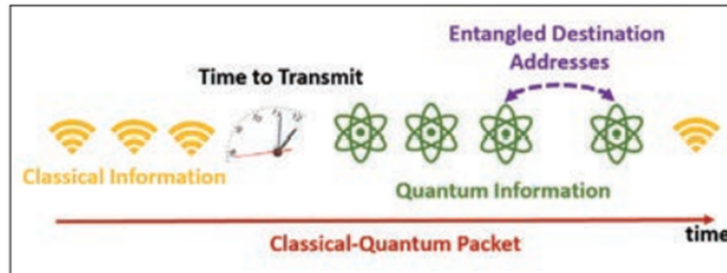


Figure: Live plot of QBER

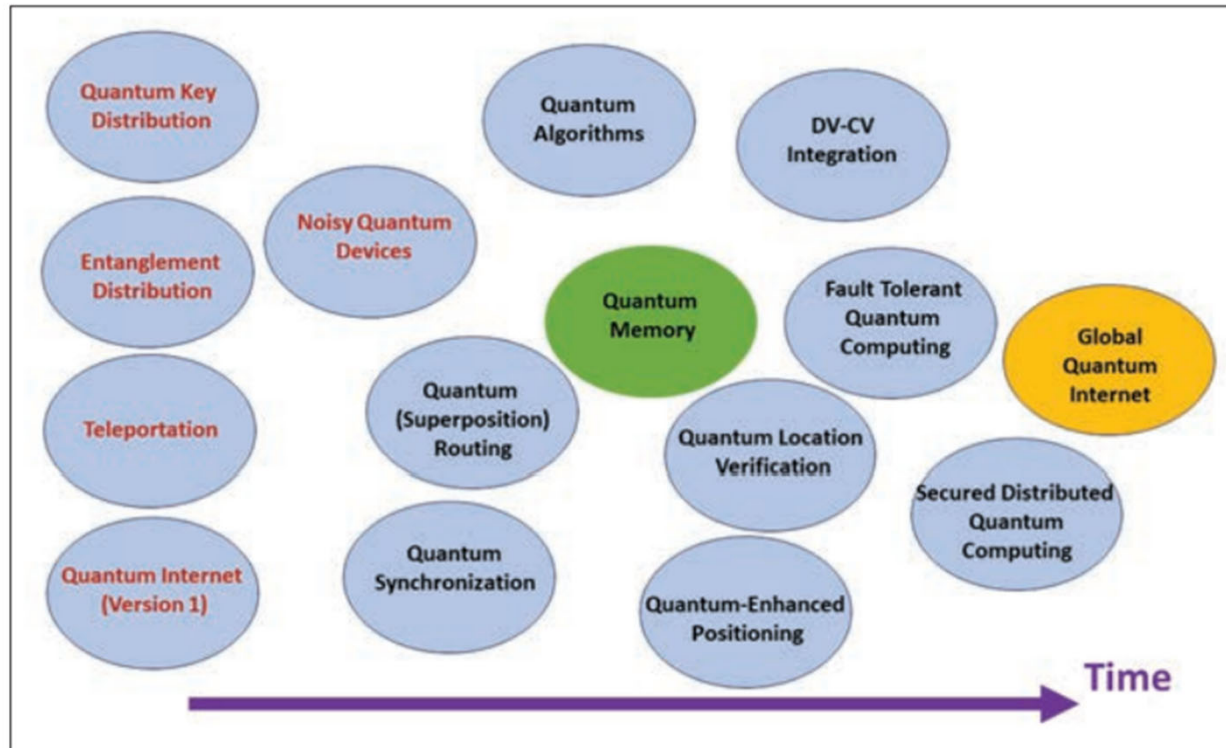
Source power (mW)	Visibility	QBER	Secure key rate (kbps)
2.5	0.960 ± 0.009	0.016 ± 0.005	1.6
3.5	0.873 ± 0.019	0.063 ± 0.009	0.7
4.5	0.742 ± 0.013	0.136 ± 0.008	Nil

Table: The experimental values for visibility, QBER, and secure key rate (kbps) at different optical powers of the EPS.

When is the Quantum Internet?



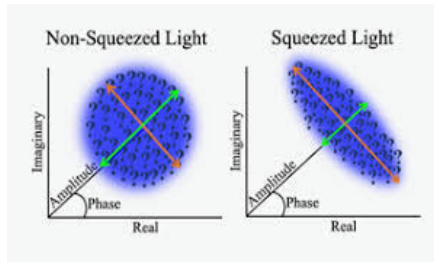
Many issues outstanding on standardisation of “quantum internet protocols” such as packet formats



Many steps outstanding on the route to the quantum internet

FIGURE 6. The Evolution of the GQI. Shown here is the estimated timeline to the full-blown GQI. The labels in red indicate the near term (current to 5 years) technical outcomes and applications. The green bubble indicates the importance of quantum memory in shaping the future Internet. The ultimate goal is shown in gold (10–20 years). The “Quantum Internet [Version 1]” simply refers to technology already implemented by the Micius quantum-enabled satellite.

Recent UNSW Quantum Sensing Projects (Gosalia et al)



Quadrature-squeezed state for satellite-based clock synchronization

doi:

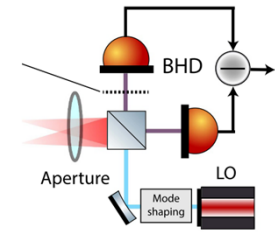
[10.1109/LATINCOM56090.2022.10000428](https://doi.org/10.1109/LATINCOM56090.2022.10000428)



Quadrature-entangled state for satellite-based clock synchronization

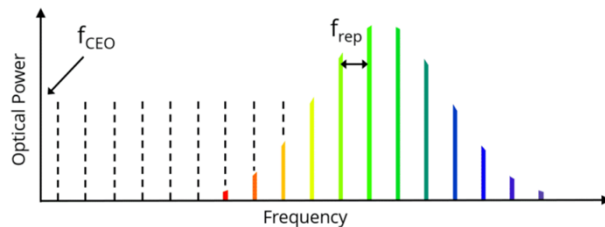
doi:

[10.1109/GLOBECOM54140.2023.10437698](https://doi.org/10.1109/GLOBECOM54140.2023.10437698)



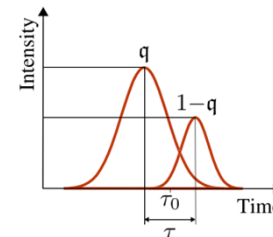
Balanced homodyne detection for sub-Rayleigh positioning of satellites

doi: [10.1088/1555-6611/ad1750](https://doi.org/10.1088/1555-6611/ad1750)



Classical and quantum frequency combs for satellite-based clock synchronization

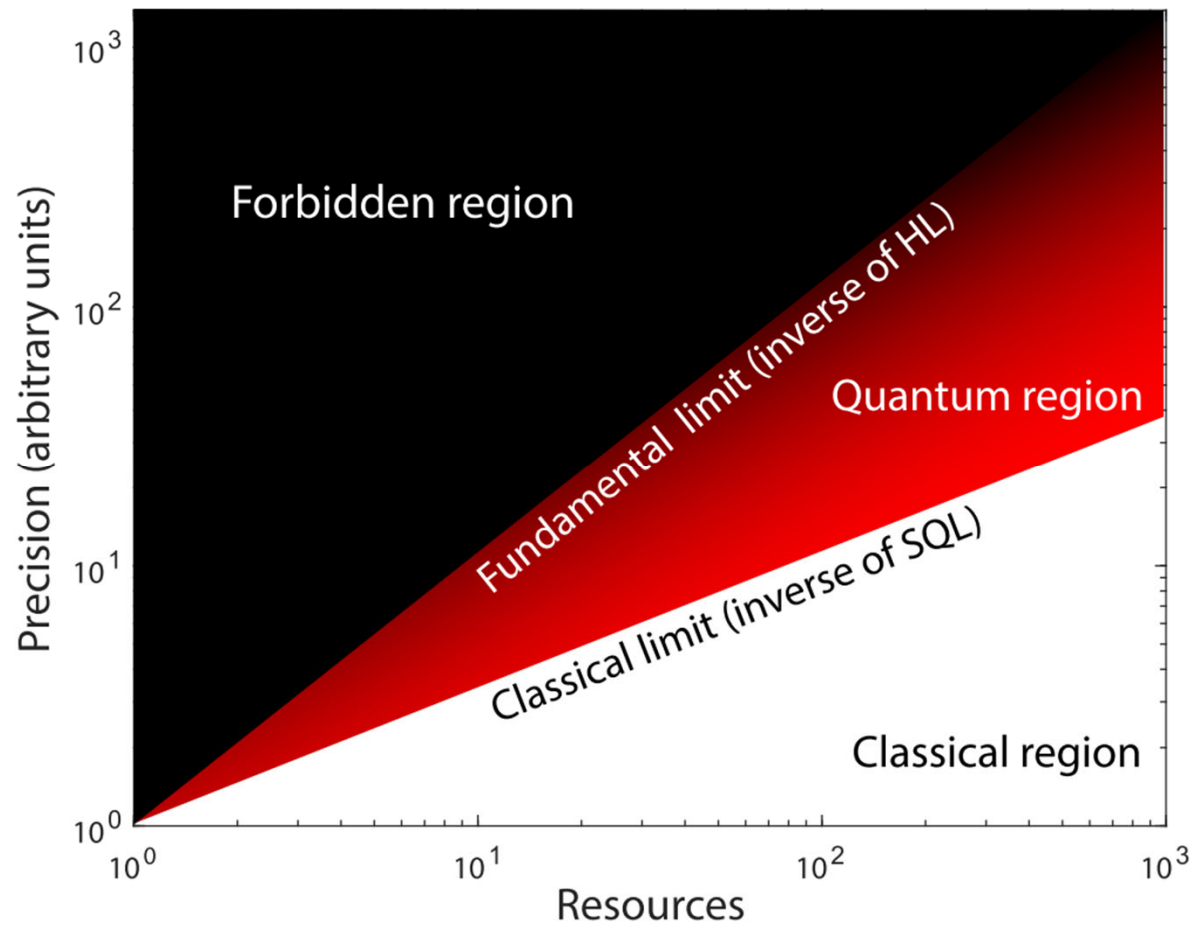
doi: [10.1063/5.0220546](https://doi.org/10.1063/5.0220546)



Fundamental analysis of the temporal mode strategy

doi: [10.1088/2058-9565/adad92](https://doi.org/10.1088/2058-9565/adad92)

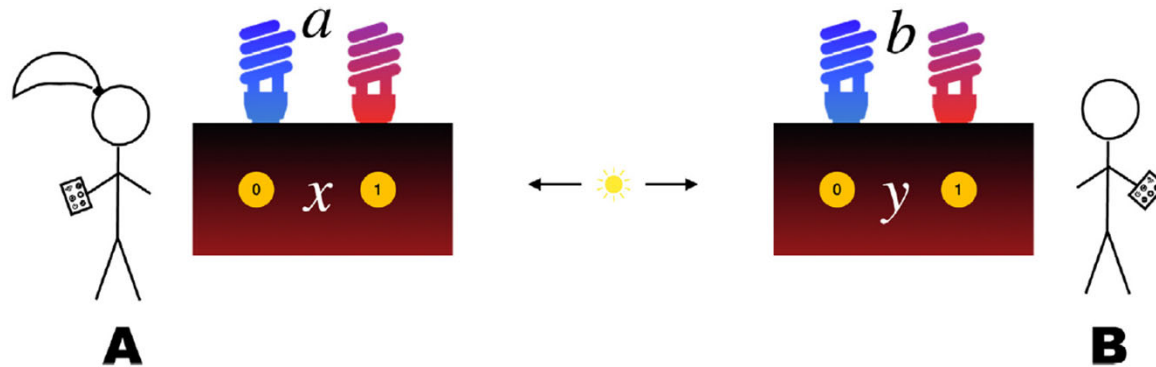
Quantum Sensing vs Classical



Fundamental Physics

A. Belenchia, M. Carlesso, Ö. Bayraktar et al.

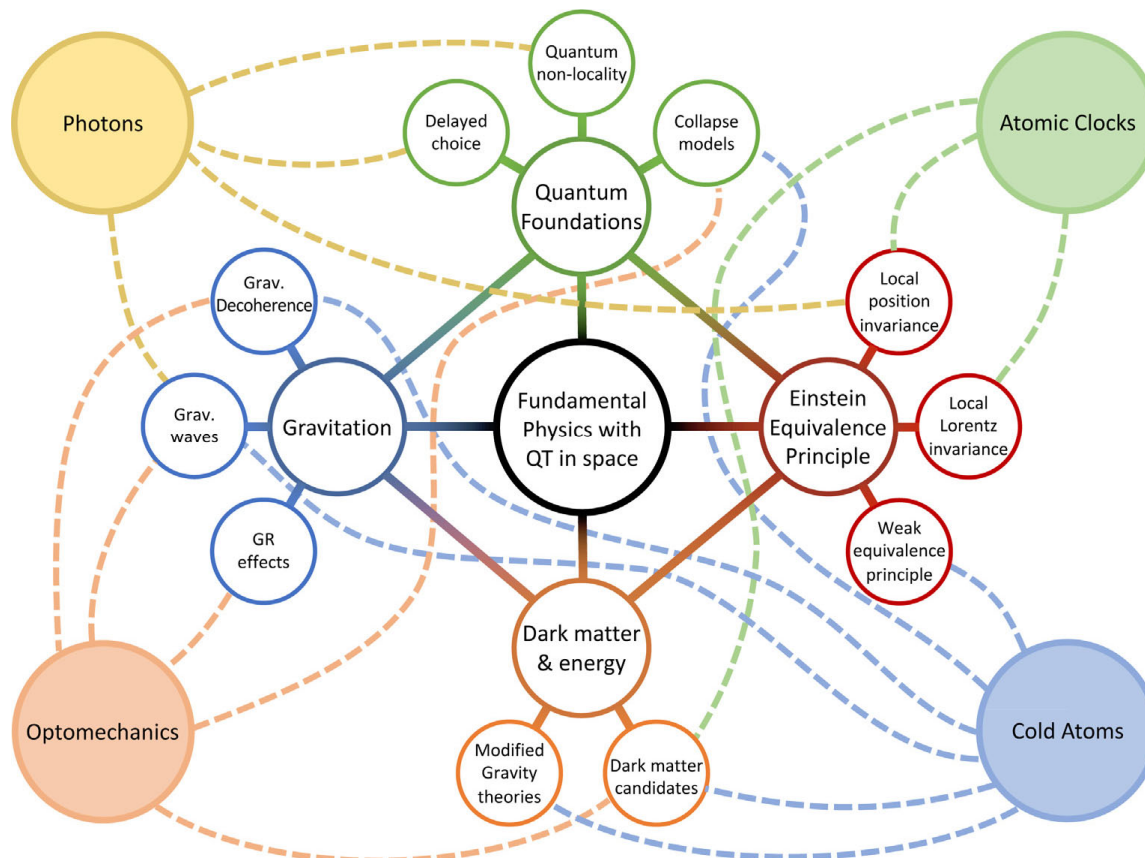
Physics Reports 951 (2022) 1–70



Bell's inequalities violations (BIV) at scale and with general relativity

NASA's Deep Space Quantum Link (DSQL), which will employ the Lunar Orbital Platform-Gateway – a space station orbiting the moon – to establish a quantum link with ground stations which will allow testing BIV

M. Mohageg, D. Strekalov, S. Dolinar, M. Shaw, N. Yu, Deep Space Quantum Link, vol. 2063, 2018, p. 3039.



Quantum Sensing Techniques

Birth correlation of entangled photons (DV)

Entanglement measurement outcomes (DV)

Derivative (higher HG) mode projections (DV and CV)

Quantum frequency combs (CV and DV)

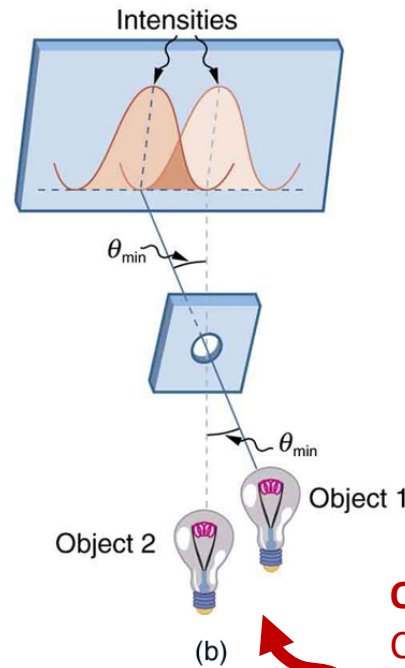
But recall scaling issues and
equal resource issues,
Equal energy ->
Quantum Cramer Rao Bounds

(Don't always discount classical)

At FFI 10^{-21} at sub-femtosecond synchronization

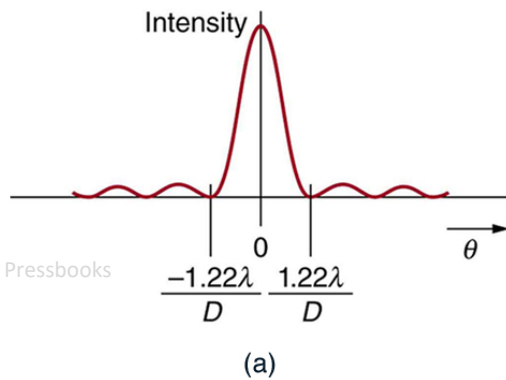
- The Einstein equivalence principle.
- The nature of fundamental physical constants.
- Dark sector physics (dark matter and dark energy).
- The possible quantum aspects of curved space-time.
- [Enhanced Engineering (PNT etc), not listed]

Defeating Rayleigh's Curse with Quantum Measurements

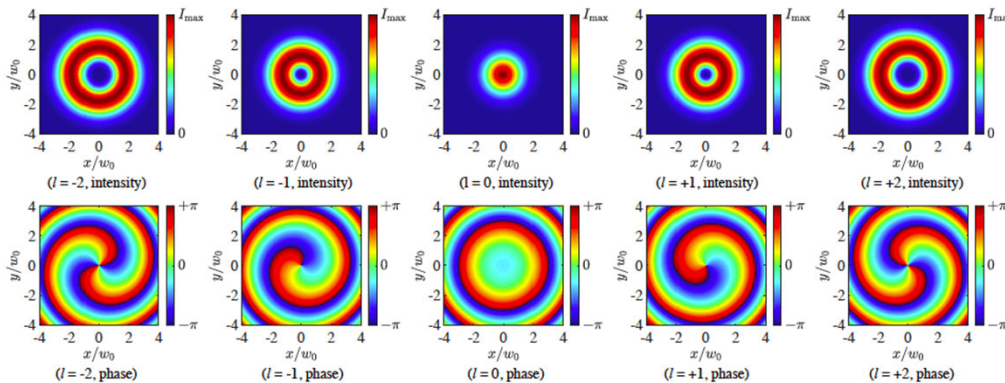


Aim:

Rayleigh curse defeated for
angle jitter less than
one part in a million

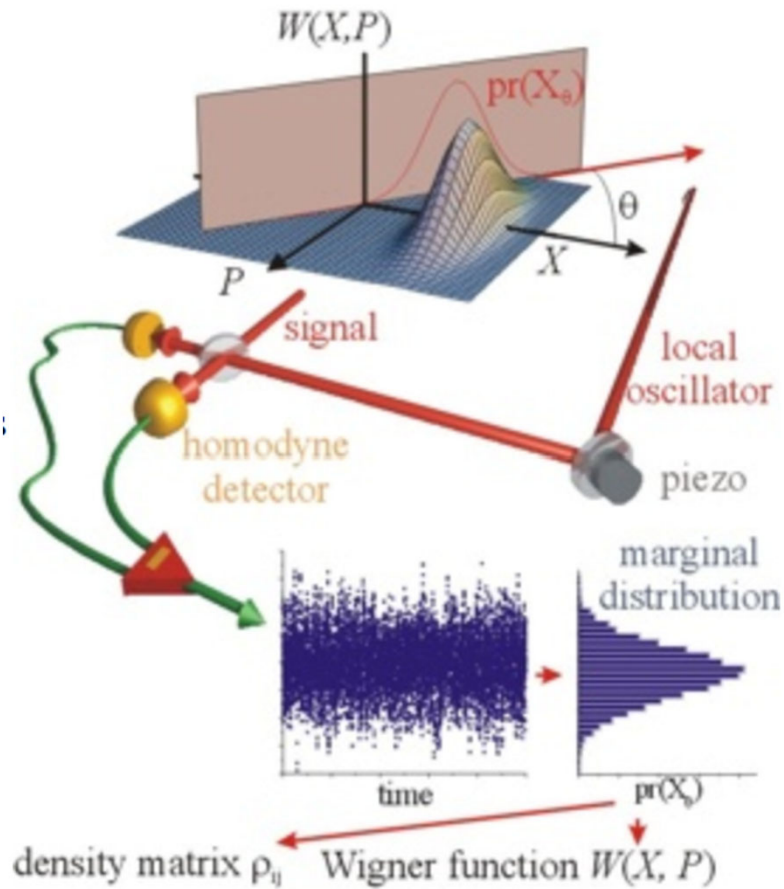


Quantum Measurement:
Count Number Photons in each
Hermite-Gaussian Modes (SPADE)

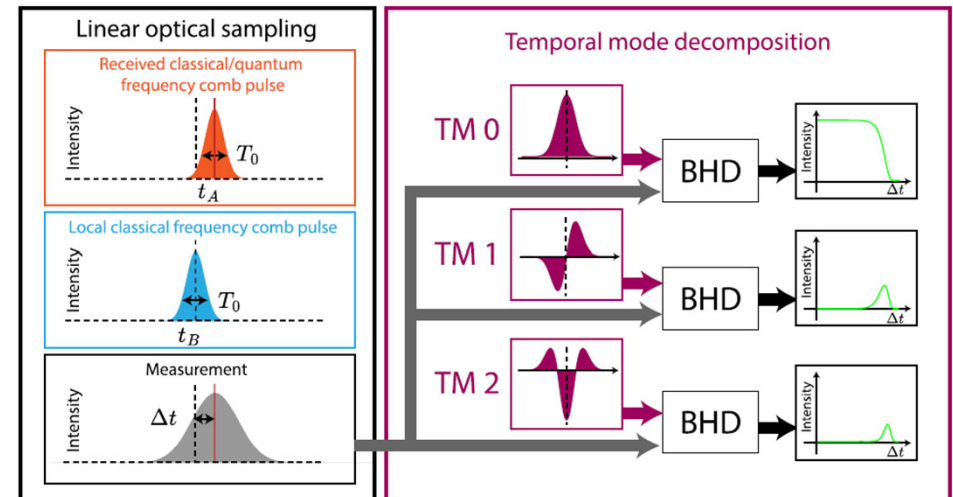


GOSALIA ET AL (NASA COLLABORATION)

Optimal Sensing Detection - Modified Homodyne

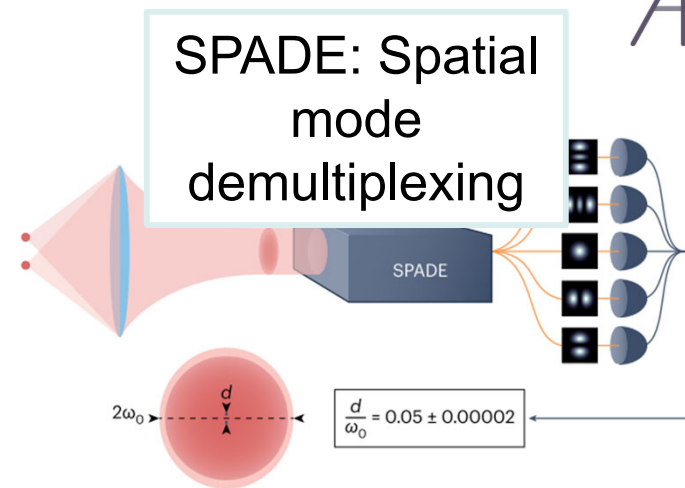
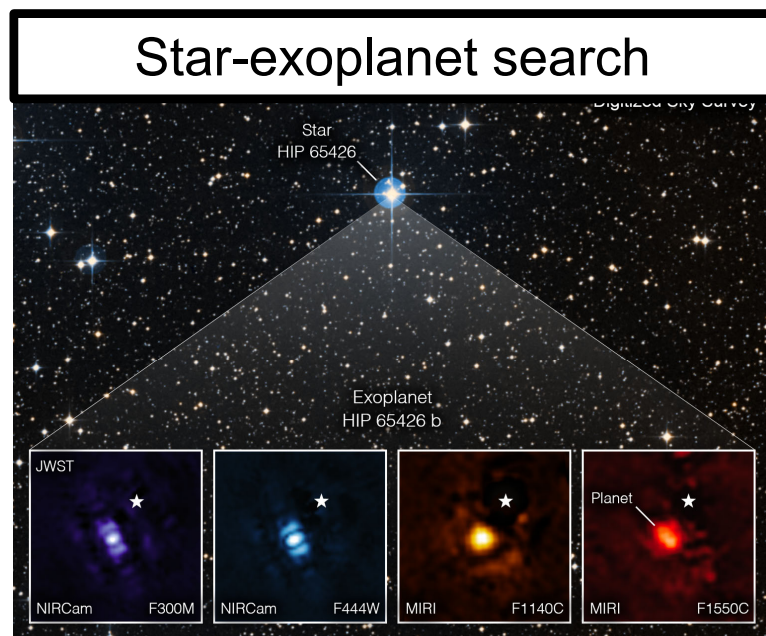


Replace local oscillator
with
derivative of “HG Modes”



Ronakraj K. Gosalia, Ryan Aguinaldo, Jonathan Green, Holly Leopardi, Peter Brereton, Robert Malaney: APL Photon. **9**, 100903 (2024); doi: 10.1063/5.0220546

Application 1 – astronomy



Resolving **two** incoherent point **sources** of light, separated by a **distance** below the Rayleigh limit

w_0 : Beam waist
 N : number of photons

As $d \rightarrow 0$

Conventional direct diffraction-limited imaging: $\sigma_d \rightarrow \infty$

SPADE: $\sigma_d \rightarrow \frac{2w_0}{\sqrt{N}}$

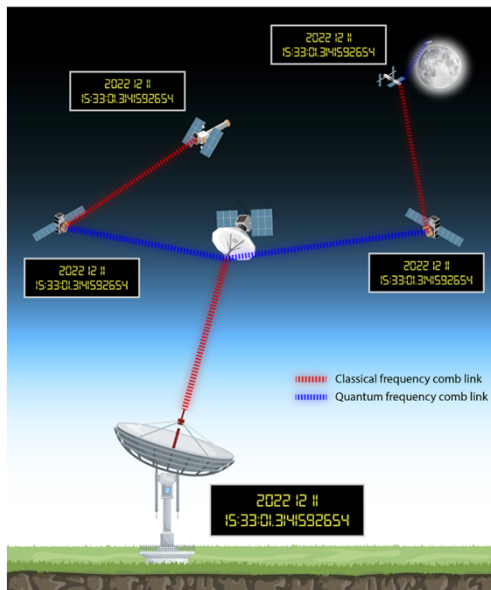
Tsang, Mankei, et al. "Quantum Theory of Superresolution for Two Incoherent Optical Sources," Phys. Rev. X, vol. 6, no. 3, Aug. 2016, p. 031033, doi:10.1103/PhysRevX.6.031033.

Phys. Rev. X, vol. 6, no. 3, Aug. 2016, p.

Application 2 – clock synchronization



Synchronizing a network of clocks

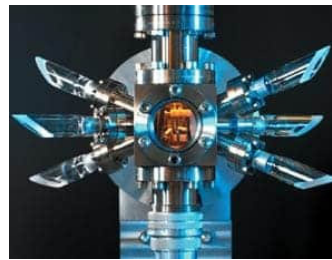


Step 1: Estimate time offset between two clocks.

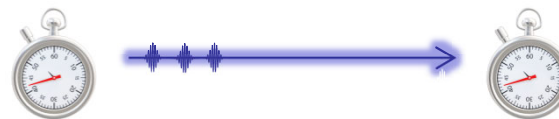
Step 2: Correct for offset.

Step 3: Wait coherence time, return to step 1.

Optical atomic clocks

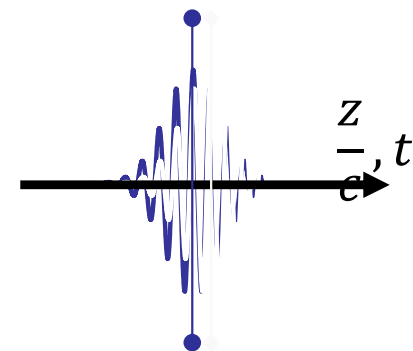


Strontium: FFI of 10^{-18} at 10^4 s
Ytterbium: FFI of 10^{-19} at 10^5 s



Pulsed laser phase-locked to clock transitions are exchanged over free space

Pulses overlapped



Pulse duration: order 100 fs
Time offset: order 1 fs

Temporal mode decomposition

Frequency Combs

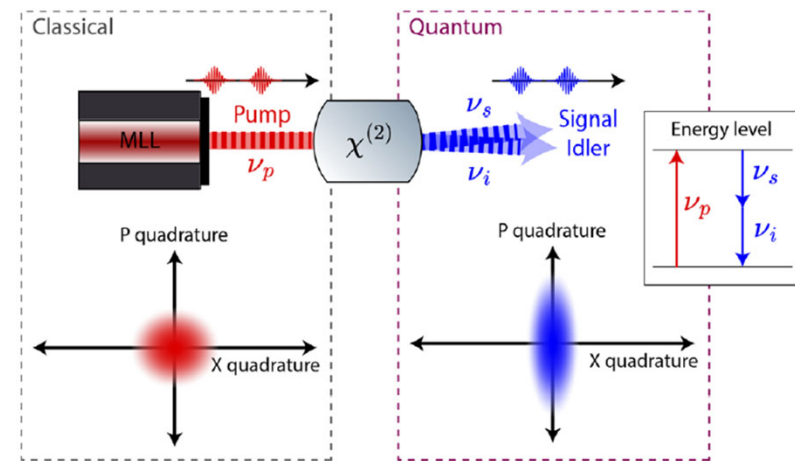
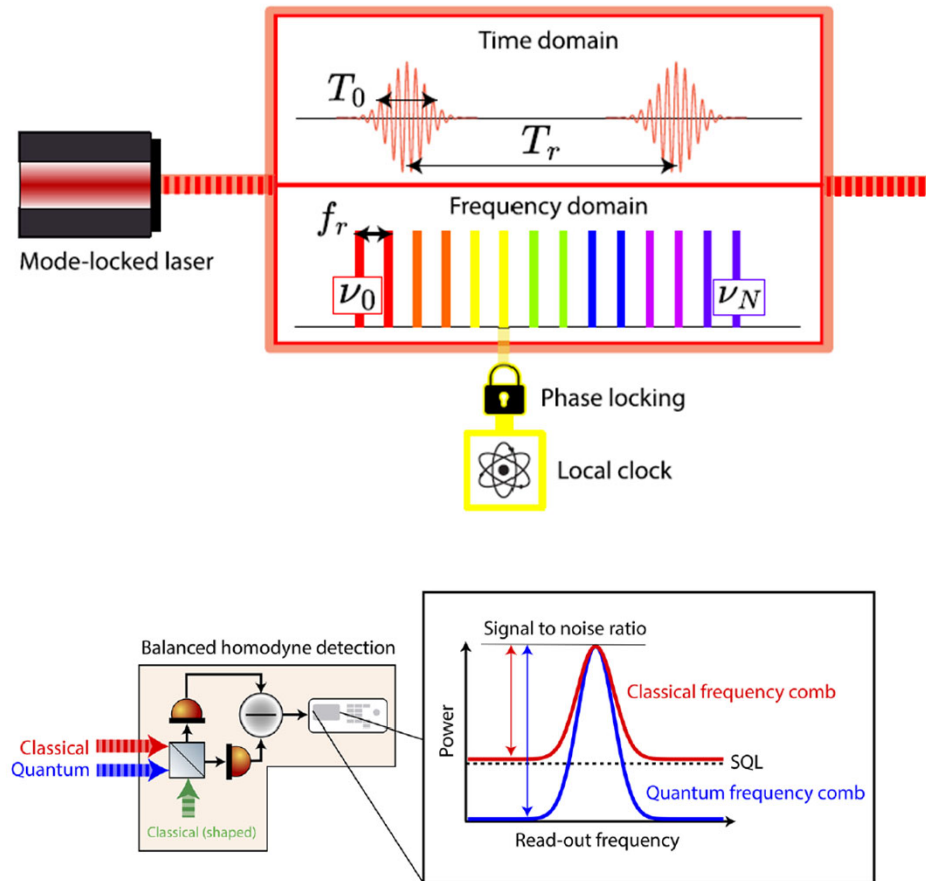
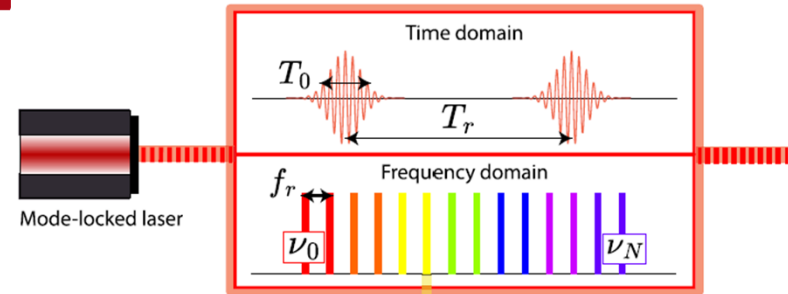


FIG. 7. Spontaneous parametric downconversion (SPDC) process is a $\chi^{(2)}$ non-linear process that can be used to convert a classical frequency comb (e.g., mode-locked laser, MLL) into a quantum frequency comb that exhibits quadrature-squeezing properties. The implementation of SPDC shown above is degenerate whereby the signal and idler have exactly half the energy (in turn center frequency) as the pump. As an example, we show the phase space diagram of the classical and quantum frequency comb with X-quadrature-squeezing. Evidently, the quantum frequency comb has reduced variance in the X quadrature and would correspondingly yield a more precise measurement than the classical frequency comb.

$$\sigma_{\Delta t, TM} \propto \frac{\exp(-r)}{\sqrt{n((1/T_0)^2 + \nu_0^2)}} \rightarrow \frac{1}{n\sqrt{(1/T_0)^2 + \nu_0^2}},$$

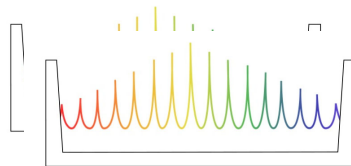
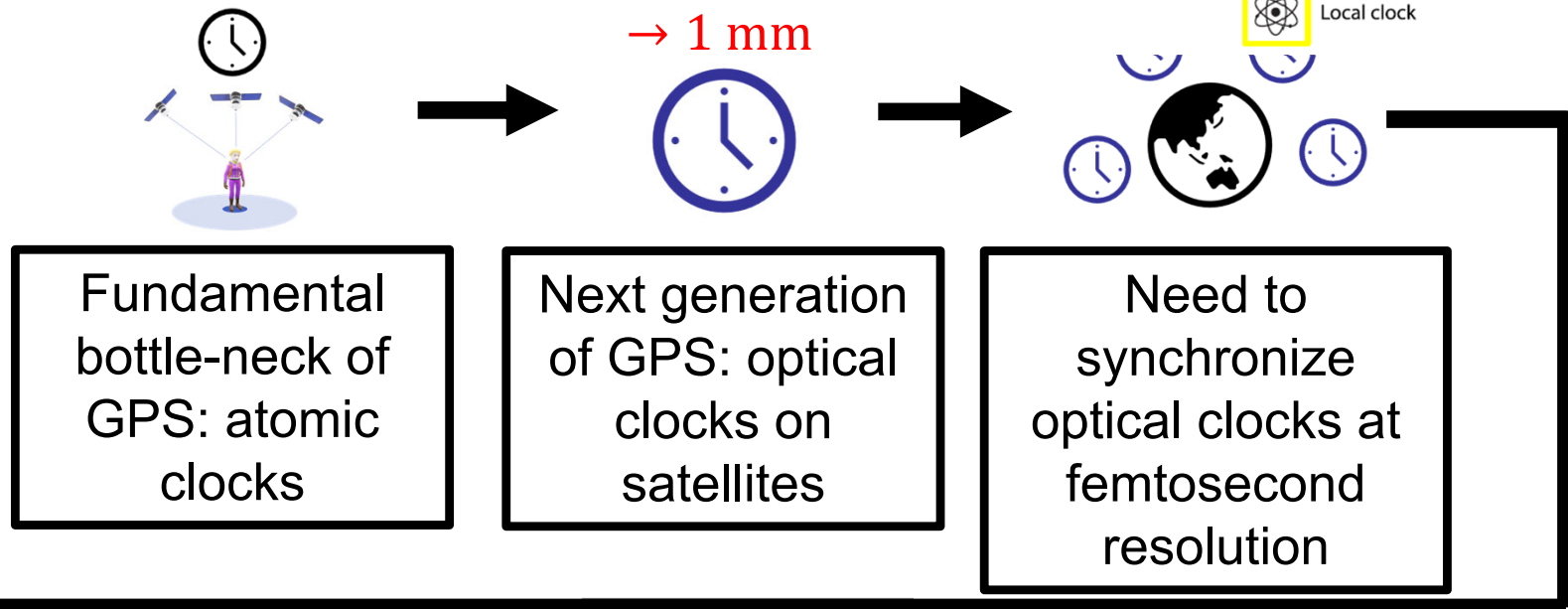
Classical and quantum frequency combs for satellite-based clock synchronization
Ronakraj K. Gosalia, Ryan Aguinaldo, Jonathan Green, Holly Leopardi, Peter Brereton
and Robert Malaney: APL Photon. **9**, 100903 (2024); doi: 10.1063/5.0220546

Frequency combs



1 m
→ 1 mm

Phase locking
Local clock



*Positioning, navigation
and timing at the
fundamental limits!*

Frequency combs enable femtosecond resolution, but have limited performance

Quantum frequency combs can reach the fundamental limit in performance

Optical frequency comb-based clock synchronization

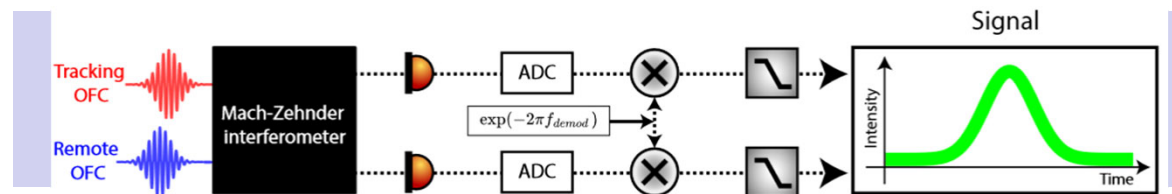
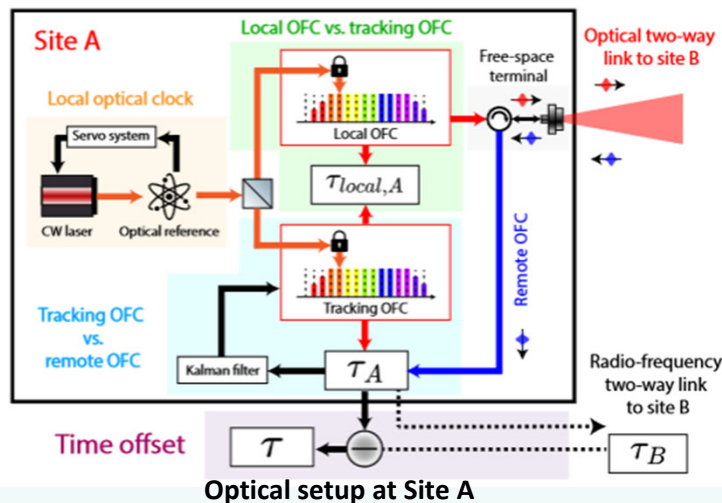
State-of-the-art clock synchronization over free-space by Caldwell et al., 2023.

Timing deviation: 300 fs after 1 second measurement time



$$\begin{aligned}\tau_A &= \tau_{B \rightarrow A} + \tau_{local,A} \\ &+ \tau/2 \\ \tau_B &= \tau_{A \rightarrow B} + \tau_{local,B} \\ &- \tau/2\end{aligned}$$

$$\begin{aligned}\tau &= \tau_A - \tau_B \\ &- (\tau_{local,A} - \tau_{local,B}) \\ &\approx \tau_A - \tau_B\end{aligned}$$



Signal generation stage: from optical frequency comb to electronic signal

State of the art

TABLE III. Recent field experiments using MLL-based classical frequency combs over optical fiber and terrestrial links and their reported performance metrics. The general trend across the recent free-space experiments has been toward longer link range, shorter integration time (τ), and an MDEV below 10^{-18} (in turn, lower TDEV).

Author	Year	Protocol	Link type	Nodes	Path (km)	MDEV	Integration time, τ (s)	TDEV (s)
Predehl <i>et al.</i> ¹³⁸	2012	OFT	Fiber	11	920	10^{-18}	10^3	6×10^{-16}
Droste <i>et al.</i> ¹³⁹	2013	OFT	Fiber	2	1840	4×10^{-19}	10^2	2×10^{-17}
Bercy <i>et al.</i> ¹⁴⁰	2014	OFT	Fiber	2	100	5×10^{-21}	10^3	3×10^{-18}
Giorgetta <i>et al.</i> ¹²	2013	O-TWTFT	Free-space	2	2	10^{-18}	10^3	6×10^{-16}
Deschenes <i>et al.</i> ¹³	2016	O-TWTFT	Free-space	2	4	5×10^{-19}	10^4	3×10^{-15}
Sinclair <i>et al.</i> ¹⁴³	2018	O-TWTFT	Free-space	2	4	10^{-17}	1	7×10^{-18}
Sinclair <i>et al.</i> ¹⁴⁵	2019	O-TWTFT	Free-space	2	4	10^{-18}	10^2	6×10^{-17}
Bodine <i>et al.</i> ¹⁴⁵	2020	O-TWTFT	Free-space	3	14	10^{-18}	10^2	6×10^{-17}
Ellis <i>et al.</i> ¹⁴	2021	O-TWTFT	Free-space	3	28	10^{-18}	2×10^2	1×10^{-16}
Shen <i>et al.</i> ²⁸	2022	O-TWTFT	Free-space	2	113	4×10^{-19}	10^4	2×10^{-15}
Caldwell <i>et al.</i> ¹⁷	2023	O-TWTFT	Free-space	2	300	5×10^{-18}	1×10^3	3×10^{-16}

In a laboratory experiment, Wang *et al.*²¹ successfully conducted temporal mode decomposition to achieve $\sigma_{\Delta t, TM}$ as per Eq. (18) with a 1.5 dB quadrature-squeezed quantum frequency comb. The setup consisted of a Ti:sapphire-based MLL that generated (ultra-short) 130 fs duration pulses with $\nu_0 = 0.25$ THz and $f_r = 75$ MHz. The remote classical frequency comb was produced using the same MLL source. The 1.5 dB of quadrature-squeezing was achieved using an SPOPO setup,^{130,148,159} which successfully reduced the $\sigma_{\Delta t}$ from 8.9×10^{-23} to 7.5×10^{-23} s. These laboratory

Gosalia et al research findings

Published in IEEE Latincom 2022

Can *quadrature-squeezing* be used on low-Earth-orbit satellites to synchronize clocks beyond the standard quantum limit?

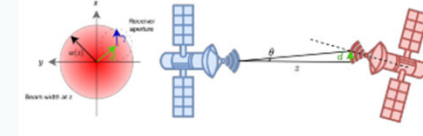
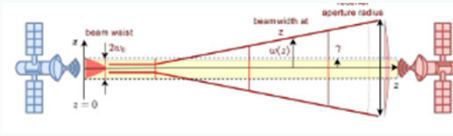
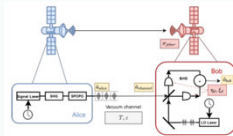
Beyond the Standard Quantum Limit in the Synchronization of Low-Earth-Orbit Satellites

Ronakraj Gosalia*, Robert Malaney*, Ryan Aguinaldo[†], Jonathan Green[‡] and Mark Clampin[‡]

* School of Electrical Engineering and Telecommunications,
University of New South Wales, Sydney, NSW 2052, Australia.

[†] Northrop Grumman Corporation, San Diego, CA 92128, USA.

[‡] NASA Goddard Space Flight Center, Greenbelt, MD 20771, USA.



Published in IEEE Globecom 2023

Can quadrature-entangled light provide any advantage over quadrature-squeezed light for clock synchronization in practice?

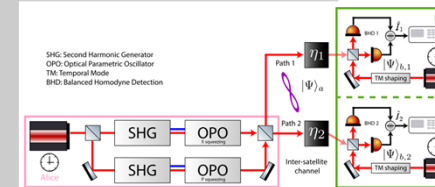
LEO Clock Synchronization with Entangled Light

Ronakraj Gosalia*, Robert Malaney*, Ryan Aguinaldo[†], Jonathan Green[‡] and Peter Brereton[‡]

* University of New South Wales, Sydney, NSW 2052, Australia.

[†] Northrop Grumman Corporation, San Diego, CA 92128, USA.

[‡] NASA Goddard Space Flight Center, Greenbelt, MD 20771, USA.



Published in IOP Laser Physics
2023

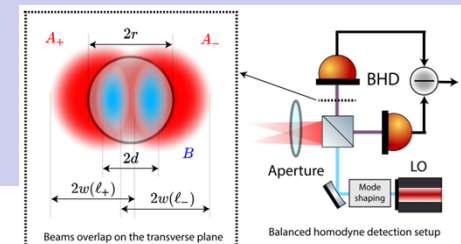
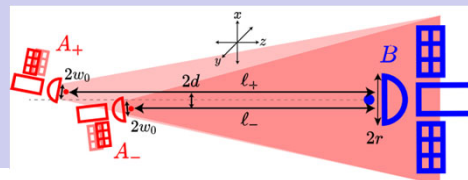
Can a 'simple' *balanced homodyne detection* setup be used to achieve super-resolution localization of satellites in low-Earth-orbit?

Quantum super-resolution with
balanced homodyne detection
in low-earth-orbit

Ronakraj K Gosalia^{1,*}, Robert Malaney¹, Ryan Aguinaldo² and Jonathan Green²

¹ University of New South Wales, Sydney, NSW 2052, Australia

² Northrop Grumman Corporation, San Diego, CA 92128, United States of America



Towards the Quantum Internet: Conclusions

- New Schemes for Quantum Communication Diversity

Enhanced
Capacity

- Use of Squeezed Light in Space for Enhanced Timing Resolution

Quantum
Sensing in
Space

- Super Resolution Telescopes via Quantum Measurements

New Space
Telescopes

- Classical and Quantum Combined Signalling

A new model for
communications

- Entangled QKD+PQS Satellite

LAUNCH 2030